Available online at www.sciencedirect.com
SCIENCE DIRECT®
Biochimica et Biophysica Acta 1661 (2004) 154–165
BIOCHIMICA ET BIOPHYSICA ACTA
BBA
www.bba-direct.com

Highly robust lipid membranes on crystalline S-layer supports investigated by electrochemical impedance spectroscopy

Petra C. Gufler, Dietmar Pum, Uwe B. Sleytr, Bernhard Schuster*

Center for NanoBiotechnology and Ludwig-Boltzmann-Institute for Molecular Nanotechnology, BOKU-University of Natural Resources and Applied Life Sciences, Vienna, Gregor-Mendel-Straße 33, 1180 Vienna, Austria

Received 6 October 2003; received in revised form 16 December 2003; accepted 22 December 2003

Abstract

In the present work, S-layer supported lipid membranes formed by a modified Langmuir–Blodgett technique were investigated by electrochemical impedance spectroscopy (EIS). Basically two intermediate hydrophilic supports for phospholipid- (DPhyPC) and bipolar tetraetherlipid- (MPL from *Thermoplasma acidophilum*) membranes have been applied: First, the S-layer protein SbpA isolated from *Bacillus sphaericus* CCM 2177 recrystallized onto a gold electrode; and second, as a reference support, an S-layer ultrafiltration membrane (SUM), which consists of a microfiltration membrane (MFM) with deposited S-layer carrying cell wall fragments. The electrochemical properties and the stability of DPhyPC and MPL membranes were found to depend on the used support. The specific capacitances were 0.53 and 0.69 μF/cm^2 for DPhyPC bilayers and 0.75 and 0.77 μF/cm^2 for MPL monolayers resting on SbpA and SUM, respectively. Membrane resistances of up to 80 MΩ cm^2 were observed for DPhyPC bilayers on SbpA. In addition, membranes supported by SbpA exhibited a remarkable long-term robustness of up to 2 days. The membrane functionality could be demonstrated by reconstitution of membrane-active peptides such as valinomycin and alamethicin. The present results recommend S-layer-supported lipid membranes as promising structures for membrane protein-based biosensor technology.

Keywords: Crystalline bacterial surface layer (S-layer); Supported lipid membrane; Impedance spectroscopy; Archaeal lipid; Valinomycin; Alamethicin

1. Introduction

In the last decade, research on functional synthetic model membranes for biosensoric devices was mainly focussed on the development of supported membranes [1–7]. The challenge is to overcome the drawbacks of conventional free-standing lipid membranes in terms of long-term robustness without impairing resistance, ionic reservoir on both sides of the membrane, and functionality by the solid support.

Recently, the biomimetic concept of applying two-dimensional crystalline bacterial surface layers (S-layers) as molecular building blocks within the scope of solid supported functional phospholipid and tetraetherlipid membranes has been introduced [8,9]. It has been demonstrated that S-layers act as a stabilizing and separating ultrathin layer that preserves the fluidity of the membrane and provides a non-denaturing environment for membrane-related functional molecules [10–12]. S-layers represent the outermost component of the cell envelope of many procaryotic organisms (archaea and bacteria) [13]. Wild-type S-layer proteins usually are isolated from purified cell wall fragments. In recent years, different kinds of genetically engineered S-layer protein species with distinct properties and specific binding domains (e.g. streptavidin) have been synthesized [14–16] offering a broad application spectrum in the field of nanobiotechnology and membrane protein-based biochip technology. The most remarkable property of isolated monomeric wild-type and recombinant S-layer proteins is their ability to self-assemble in suspension, on various solid supports (e.g. gold, silicon), at the air/water interface, on Langmuir lipid films, on bilayer lipid membranes and on liposomes [13]. In gram-negative archaea, the crystalline S-layer is the only cell wall component external to the cytoplasmic membrane

* Corresponding author. Univ. fur Bodenkultur Wien, Zentrum Ultrastrukturforschung, Gregor-Mendel-Strasse 33, Vienna A-1180, Austria. Tel.: +43-1-47654-2213; fax: +43-1-4789112.
E-mail address: bernhard.schuster@boku.ac.at (B. Schuster).

0005-2736/$ - see front matter © 2004 Elsevier B.V. All rights reserved.
doi:10.1016/j.bbamem.2003.12.009

[17]. In contrast to bacterial S-layers, domains of the polypeptide-chain of many archeal S-layers are integrated into the hydrophobic core of the cytoplasmic membrane [17]. In the course of evolution, archaea have developed unique membrane lipids due to their extreme environments [18]. Their cytoplasmic membrane mainly consists of bolaamphiphilic membrane-spanning glycerol ether lipids, resulting in a remarkable stability and very good insulating properties [18,19].

In this study, the well-characterized S-layer protein SbpA from *Bacillus sphaericus* CCM 2177 [8,20] was used as an ultrathin crystalline, water-containing hydrophilic layer between a gold electrode and the membrane. For SbpA a square lattice with a lattice constant of 13.1 nm has been determined [21]. One morphological unit ($A \sim 170$ nm^2) consists of four protein monomers. The pores are of identical size and morphology with a diameter of ~3.5 nm [21]. One protein subunit has a relative molecular weight of ~127,000 [20]. The thickness of an SbpA lattice is ~8 nm [22]. The randomly oriented crystallites had a crazy-paving appearance and reached an average size of 0.1–1 μm in diameter. With regard to their orientation in vivo, a common feature of S-layers of many Bacillaceae is their smoother, charge-neutral outer surface and a more corrugated, net-negatively charged inner surface [9]. The N-terminus of the polypeptide-chain, which is located on the inner surface, contains at least one S-layer homologous motif that anchors the SbpA monomer via the secondary cell wall polymer to the rigid peptidoglycan layer [22,23]. SbpA recrystallizes in monomolecular lattices with the charge-neutral outer surface exposed to the aqueous solution and the net-negatively charged inner surface attached to the gold (Neubauer, A., Györvary, E.S., personal communication).

The motivation of the present work was the implementation of electrochemical impedance spectroscopy (EIS) as an investigative tool for S-layer supported biomimetic membranes. In order to mimic the supramolecular architecture of the archaeal cell envelope, the commonly used synthetic phospholipid DPhyPC and the bolaamphiphilic main tetraether phospholipid (MPL) isolated from *Thermoplasma acidophilum* have been chosen for membrane formation. As there are serious difficulties in isolating archaeal S-layer proteins due to the tight interaction of hydrophobic domains of the S-layer and the lipids (e.g. use of detergent is required), no detailed procedure for recrystallization of archaeal S-layer proteins on surfaces and interfaces is available, and thus, SbpA isolated from gram-positive *B. sphaericus* was used. EIS has been applied to probe the physical properties of functionalized supported lipid membranes [24–28]. Further on, S-layer ultrafiltration membranes (SUMs) and microfiltration membranes (MFMs) have been used as reference supports to the recrystallized SbpA lattice. An SUM is composed of a polyamide MFM, where S-layer fragments of *B. sphaericus* CCM 2120 were deposited. The latter S-layer protein is known to be very similar to SbpA. Finally, chemical cross-linking of the S-layer fragments was performed using glutaraldehyde [29,30]. In order to approve the functionality of the membranes, reconstitution experiments using the membrane-active peptides valinomycin and alamethicin were performed.

2. Materials and methods

2.1. Chemicals

The phospholipid 1,2-diphytanoyl-*sn*-glycero-3-phosphatidylcholine (DPhyPC, Avanti Polar Lipids, Alabaster, AL) and the main tetraether phospholipid of *T. acidophilum* (MPL, Matreya, Inc., Pleasant Gap, PA) were dissolved and stored at −20 °C in *n*-hexane/absolute ethanol (9:1, v/v, both Merck, Darmstadt, Germany) at a concentration of 10 mg lipid/ml. Their chemical structures are illustrated in Fig. 1. Buffer solutions were prepared in Milli-Q-water (Millipore, minimum resistance >18 MΩ cm), thoroughly degassed and filtered through a 0.2-μm filter (Sartorius AG, Göttingen, Germany) before use. As a standard buffer for electrochemical measurements, an aqueous solution of 10 mM Tris (pH = 7.4) containing 50–100 mM NaCl and KCl, respectively, was used. All chemicals were purchased from Sigma-Aldrich (Vienna, Austria).

2.2. Preparation of gold subtrates

Glass microscope slides (ELKA, Germany) were cut into half and cleaned by ultrasonic treatment twice for 15 min in 2% Hellmanex (Hellma, Müllheim, Germany) and twice for 15 min in absolute ethanol. After each ultrasonication step, the slides were rinsed thoroughly in Milli-Q-water. Finally, they were dried in a stream of nitrogen. Subsequently, a 100-nm thin layer of gold was deposited onto the glass (sputter coater SCD 004, Balzers, Lichtenstein). Before the recrystallization of S-layer proteins, the substrates were stored in clean air for approximately 2 days.

2.3. Isolation and recrystallization of S-layer proteins

Growth, cell wall preparations, and extractions of the S-layer protein SbpA isolated from *B. sphaericus* CCM 2177 (Czech Collection of Microorganisms) were performed as described elsewhere [31]. The SbpA stock solution was diluted with 0.5 mM Tris (pH = 9) containing 10 mM $CaCl_2$ to a final concentration of 0.1 mg/ml. The gold substrates were immersed into the solution and recrystallization was performed over night (18 h). SbpA-coated gold substrates were stored in Milli-Q-water at 4° until usage. Atomic force microscopical (AFM) investigations (Nanoscope III, Digital Instruments Inc., Santa Barbara, CA) were performed to confirm the entire coverage of the gold surface with a crystalline SbpA lattice. In some experiments, the SbpA

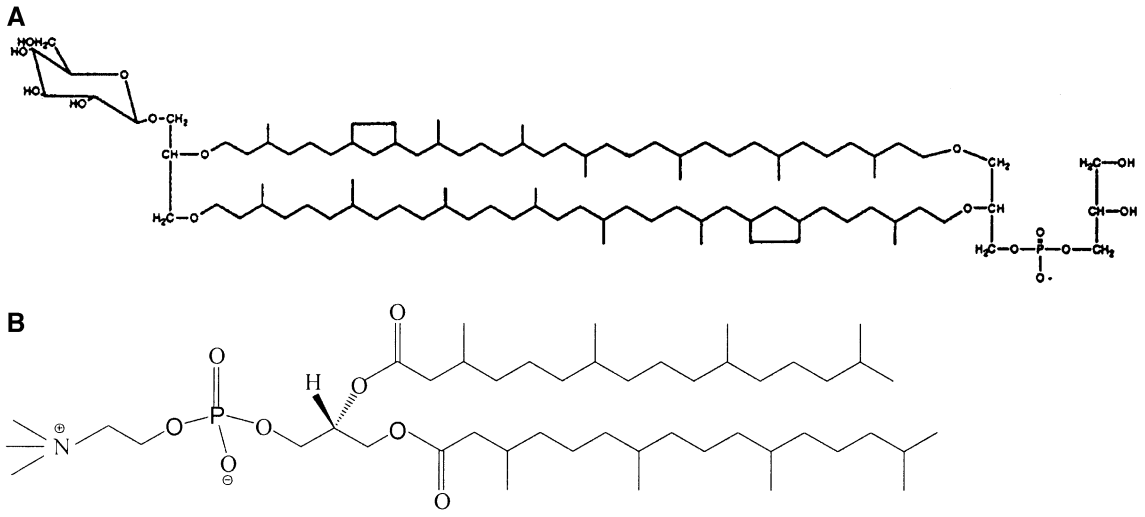

Fig. 1. Chemical structure of (B) the phospholipid DPhyPC and (A) the bolaamphiphilic main tetraether phospholipid (MPL) isolated from *T. acidophilum*.

lattice was cross-linked with glutaraldehyde (20 min; 0.5% glutaraldehyde in 100 mM phosphate-buffer, pH 7.5).

2.4. Production of SUMs

B. sphaericus CCM 2120 was obtained from Czech Collection of Microorganisms (CCM), Brno, Czech Republic. To produce SUMs, S-layer carrying cell wall fragments were deposited on MFMs with an average pore size of 0.4 μm (SM 25058, Sartorius) as described elsewhere [29,30]. SUMs were stored in Milli-Q-water containing 50 mM NaN_3 (Merck) at +4 °C. The integrity of the ultrafiltration layer which consisted of the S-layer fragments was checked by filtration of a ferritin solution as previously described [32]. All SUMs used showed a closed defect-free ultrafiltration layer.

2.5. Formation of S-layer-supported phospholipid and tetraetherlipid membranes

A sheet of polyethylene plastic (Saran Wrap, DowBrands Inc., Canada) was attached vertically to the open side of the home-made measuring chamber (Fig. 2). The contact area between the sheet and the chamber was sealed with silicone paste (Bayer AG, Leverkusen, Germany). An orifice was made through the plastic sheet by punching with a perforating tool (0.4 mm in diameter) [33]. The orifices showed an area of $(1.0 +/- 0.29) \times 10^{-3}$ cm^2 as determined by light microscopy. An SbpA-coated gold substrate (test electrode) was placed over the aperture with the S-layer pointing toward the compartment (Fig. 2). For SUM-supported membranes, a piece of SUM (15 × 15 mm) was placed over the aperture between the plastic sheet and the gold electrode. The side of the ultrafiltration membrane with attached S-layer lattices was facing the compartment. After fixing the substrate, the chamber was filled to just above (for DPhyPC) or below (for MPL) the aperture with electrolyte and was placed into a Faraday cage. The lipid stock solution was diluted 1:20 with *n*-hexane/absolute ethanol (9:1, v/v). Subsequently, 2 μl of the diluted lipid solutions was spread on the aqueous surface. The membranes were generated by a modified Langmuir–Blodgett technique by transferring the DPhyPC monolayer twice over the aperture by lowering and raising the electrolyte level [11]. With MPL simply one raising step of the lipid monolayer was sufficient [12]. Membrane formation was confirmed by impedance spectroscopy. After each experiment, the measuring cell was cleaned extensively with 2% Hellmanex, methanol, ethanol, rinsed in Milli-Q-water and finally dried for 30 min at 60 °C.

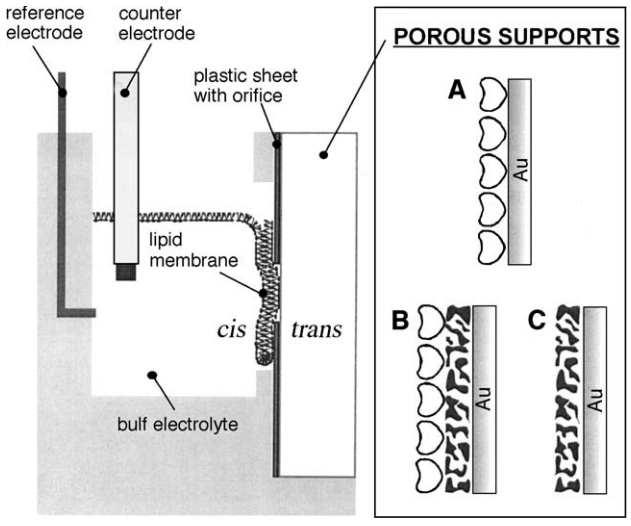

Fig. 2. Schematic drawing of the three-electrode measurement set-up with different porous supports (not drawn to scale). MPL and DPhyPC membranes were generated (A) on a closed lattice of the S-layer protein SbpA recrystallized on a gold test electrode, (B) on an S-layer ultrafiltration membrane (SUM), and (C) on a bare nylon MFM. The membrane separates the bulk electrolyte solution (*cis*) from the ionic reservoir (*trans*) within the porous supports.

2.6. Incorporation of valinomycin and alamethicin

Membrane-active peptides such as the potassium-selective ion carrier valinomycin and the voltage-dependent channel-forming peptide alamethicin were used for the functionalization of the membranes. The peptides were injected with a syringe from an ethanolic stock solution into the electrolyte to a final concentration of 4×10^{-7} M for valinomycin (Sigma) and 0.1–1 μg/ml for alamethicin (Sigma). The content of ethanol was kept very low and, thus, did not interfere with the reconstitution process or changing the resistance of the membrane. Amiloride stock solutions were prepared for alamethicin channel inhibition experiments. Amiloride–HCl·H_2O and 5-(*N*-ethyl-*N*-isopropyl)-amiloride (both Sigma) were dissolved in Milli-Q-water to a final concentration of 2 mM and stored at 4 °C until usage.

2.7. EIS

The electrical properties of S-layer-supported lipid membranes were investigated with an impedance analyser (IM6, Zahner Electronics, Kronach, Germany). All data were recorded with the IM6-Thales software. A self-made reference electrode (Ag/AgCl-wire in 2.5% agarose gel prepared in 1M KCl), a platinum counter electrode and the gold substrate as the test electrode were used to form a three-electrode-system (Fig. 2). Impedance spectra were recorded in a frequency range from 10 mHz to 100 kHz. Not the whole frequency range was used in each measurement. A small AC sinusoidal voltage of 10 mV between the test electrode and the reference electrode was applied and the system's current response was measured. Additionally, DC bias voltages of −800 to +800 mV were applied between the test electrode and the counter electrode. The polar Bode plot and the complex Nyquist plot were used to represent impedance spectra. For data analysis, the Zview2 program (Scribner Associates, Inc.) was used.

Electrochemical parameters such as membrane resistance and capacitance were obtained by fitting the data to an appropriate equivalent circuit. Knowing the membrane capacitance Cm, the thickness *d* of the hydrophobic core of the membrane can be estimated using the following equation:

$$d = \varepsilon\varepsilon_0 A/Cm \quad (1)$$

where *d* [m] is the thickness of hydrocarbon chains of the membrane, ε_0 ($=8.854 \times 10^{-12}$ [F/m]) is the dielectric constant of free space, ε ($=2.1$) is the relative dielectric constant, *A* [m^2] is the membrane area and Cm [F] is the membrane capacitance. The fitting procedure is also described in Section 3.2.1 by means of an example.

Statistical analysis was performed using the ORIGIN 6.1G software (OriginLab Corporation, Northampton, MA). All experiments were performed at room temperature (22 +/− 2 °C).

3. Results and discussion

3.1. S-layer supports

In the present study, the S-layer protein SbpA of *B. sphaericus* CCM 2177 was recrystallized on a gold surface to provide an isoporous water-containing intermediate layer between the solid support and the membrane. For the deposition of a lipid bilayer with optimal electrical properties, a defect-free large-scale protein layer of crystalline arrays is required. AFM studies revealed a homogeneous, coherent SbpA lattice that covered the entire gold surface (Fig. 3C–D). The surface roughness was determined by section analysis and revealed 3–7 nm for the bare gold and 0.3–1.1 nm (1.7 nm as a maximum value) after S-layer recrystallization. Thus, the SbpA-coated gold surface exhibited a significant smoother topography compared to bare gold (Fig. 3A–B). In some experiments, the freshly recrystallized SbpA lattice was treated with glutaraldehyde (GA) for stabilization purposes on the one hand, and the production of an S-layer surface comparable to the surface of an S-layer ultrafiltration-membrane (SUM) on the other hand. As GA cross-links the inter- and intramolecular aminogroups of proteins, only the negatively charged carboxy-groups remain on the protein [30,32]. Therefore, the surface of an SUM as well as the GA-fixed SbpA lattice were negatively charged, whereas an untreated SbpA lattice exhibited a charge-neutral surface. As asserted by AFM, the treatment of SbpA with GA did not have any impact on the topography of the crystalline lattice. We used the bare MFM as an intermediate layer for membrane formation as well. Successful application of SUMs and MFMs as supports for lipid membranes within the scope of voltage clamp experiments were described previously [11].

3.2. Characterization of S-layer-supported membranes with EIS

3.2.1. Data evaluation and fitting procedures

Membranes were generated by a modified Langmuir–Blodgett technique [12]. The great advantage of this method is a fast and reproducible formation of membranes on hydrophilic protein-supports with electrical properties comparable to classic free-standing black lipid membranes (BLMs). EIS was applied to probe the capacitive and resistive behaviour of DPhyPC and MPL membranes on SbpA, SUM and MFM supports. In an impedance spectrum, different characteristic electrical elements (resistors and capacitors) dominate along the different frequency domains. These elements are connected to an electrical equivalent circuit to which the experimental data are fitted [34]. A physical model often used to qualify supported membranes combines the electrolyte resistance Rel at high frequencies in series with a parallel assembly of membrane resistance Rm and membrane capacitance Cm in the mid frequency range, followed at lower frequencies by a serial linkage of

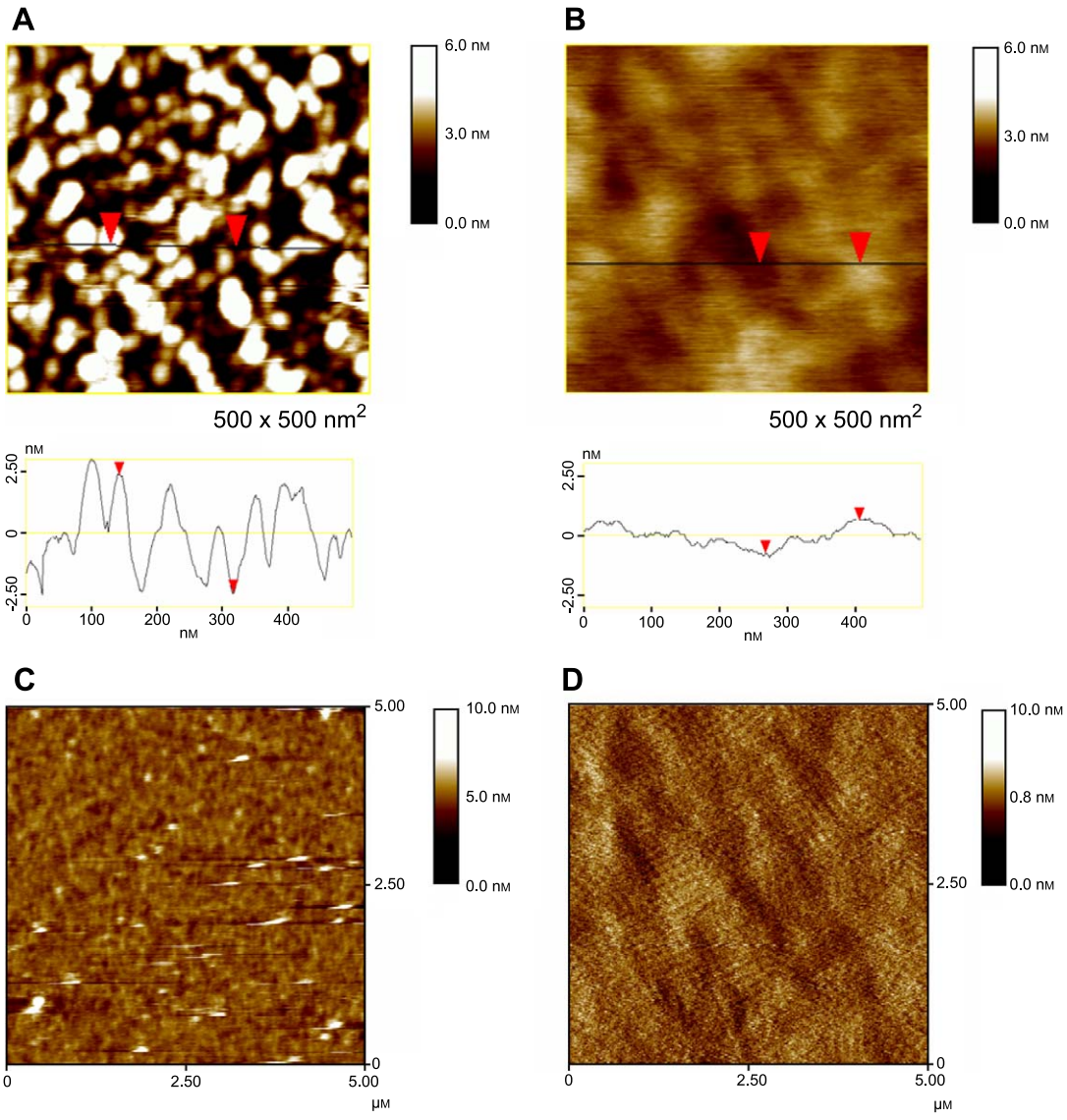

Fig. 3. AFM images of sputtered gold surface and the S-layer protein SbpA recrystallized on gold. Images were recorded in contact-mode in liquid (100 mM NaCl). (A) Height-image (Z-range = 6 nm) of the bare gold electrode. The section analysis revealed a surface roughness of 3 – 7 nm. (B) Height image (Z-range = 6 nm) of a recrystallized SbpA layer lattice. The average surface roughness was 0.3 – 1.1 nm (maximum values ~ 1.7 nm). (C) Height image (Z-range = 10 nm) of a larger S-layer-coated gold area. (D) Deflection image (Z-range = 1.5 nm) of the crystalline square lattice of SbpA (lattice constant = 13.1 nm).

Cdl, which is the electric double layer (Helmholtz) capacitance at the gold/electrolyte interface [25,35–37]. The Helmholtz capacitance strongly depends on the capacity of the ionic reservoir [25,38,39] and revealed a typical value of ~ 40 μF/cm^2 in the lower frequency domain [24,25]. In contrast to supported lipid membranes, impedance spectra of free-standing BLMs did not exhibit a Helmholtz capacitance [40]. All used supports are highly porous and electrolyte containing structures. Thus, the S-layer lattice between saran wrap and gold electrode did not only constitute a considerable ionic reservoir, but allows also that the whole gold electrode may be utilized for ion transport. Due to the configuration of the measurement cell used in our experiments (Fig. 2), there was no limitation of the gold electrode area and the ionic reservoir (electrolyte in pores of SbpA, SUM and MFM). The area of the gold electrode was very large (~ 1.5 cm^2) compared to the orifice in the plastic sheet [(1.0 +/– 0.29) × 10^{-3} cm^2], which connected the ionic reservoir (*trans*-side) with the aqueous bulk solution (*cis*-side). Thus, no distinct measurable ionic double layer at the gold/electrolyte interface was formed in the measured frequency range. In impedance spectra of the composite, various porous support/gold-structures before membrane formation, the electrolyte resistance Rel dominated the whole frequency range. At lower frequencies (< 10^{-2} Hz), a tendency to capacitive behaviour (Cdl) was observed (data not shown). Consequently, a simple analogue model circuit (Fig. 4) of a capacitor Cm in parallel with a resistor Rm was chosen for data fitting to determine capacitance and resistance of supported membranes. For a better understanding,

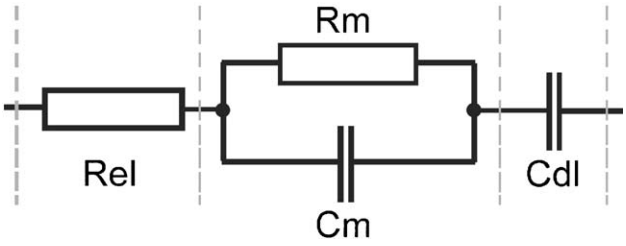

Fig. 4. Simple analogue electrical model circuit of an S-layer-supported lipid membrane. The electric elements, which were not considered within the fitting procedure (Rel, Cdl), are drawn in brackets.

the electric elements, which were not considered within the fitting procedure (Rel, Cdl), were drawn in brackets. Fig. 5A shows impedance spectra of a DPhyPC membrane on an SbpA lattice with and without reconstituted alamethicin channels. The whole frequency range was dominated by Cm (=0.55 μF/cm^2) in the curve of the non-conducting membrane (open squares). Therefore, the electrolyte resistance Rel was neglected. In most cases, the membrane was still capacitive at low frequencies, although the phase already showed a slight downward tendency (Fig. 5A). If the fitting procedure led to a high fitting error for Rm (60–100%), whereas the fitting error of Cm was below 2%, the curve was first fitted to the given equivalent circuit and Cm was determined. In a next step, an impedance simulation curve over an extended frequency range of 1 mHz–100 kHz was performed by using the previously determined Cm value. Rm was determined by adjusting the simulation curve visually to the experimental curve (continuous curve in Fig. 5A; Rm (sim)=80 MΩ cm^2). Fitted Rm values were considered in the evaluation as long as the fitting error was below 10%. In addition, instead of simulating Rm, the admittance at 0.1 Hz may be determined as a lower limit for the membrane conductivity [25].

3.2.2. Resistance, capacitance and thickness

A summary of the obtained EIS data (capacitance Cm, resistance Rm, conductivity at 0.1 Hz and thickness d of the hydrophobic membrane core) and corresponding voltage-clamp data of free-standing [12,41] and SUM supported [12] DPhyPC and MPL membranes are given in Table 1. DPhyPC membranes on SbpA showed capacitances of 0.53 +/− 0.14 μF/cm^2, resistances up to 80 MΩ cm^2 and conductivities of 0.36–0.61 μS/cm^2 at 0.1 Hz. SUM-supported DPhyPC membranes showed slightly higher capacitances (0.69 ± 0.04 μF/cm^2) and conductivities (0.49–0.63 μS/cm^2 at 0.1 Hz) and lower membrane resistances (up to 50 MΩ cm^2), whereas Cm values of voltage-clamped SUM-supported DPhyPC membranes [12] were slightly lower (Cm=0.62 ± 0.03 μF/cm^2). Folded DPhyPC bilayers (solvent: *n*-hexane/ethanol) supported by SbpA were slightly thicker (3.5 +/− 0.7 nm) and those resting on a SUM (2.7 +/− 0.2 nm) were equal than painted membranes out of squalene (2.6–3.0 nm). Painted DPhyPC membranes out of *n*-decane revealed with 4.5 nm the highest thickness. The specific capacitance, and hence the resulting thickness, is known to depend on the type of solvent used for bilayer formation. A certain amount of solvent, like *n*-decane, is present within the gap of the two hydrophobic ends of the bilayer leaflets and yields in a higher thickness [42]. In contrast, painted bilayers formed out of squalene are solvent-free, because squalene is not soluble in the bilayer [43]. In comparison to solvent-containing bilayers, folded lipid bilayers contain very little solvent; however, they are not entirely solvent-free [44,45].

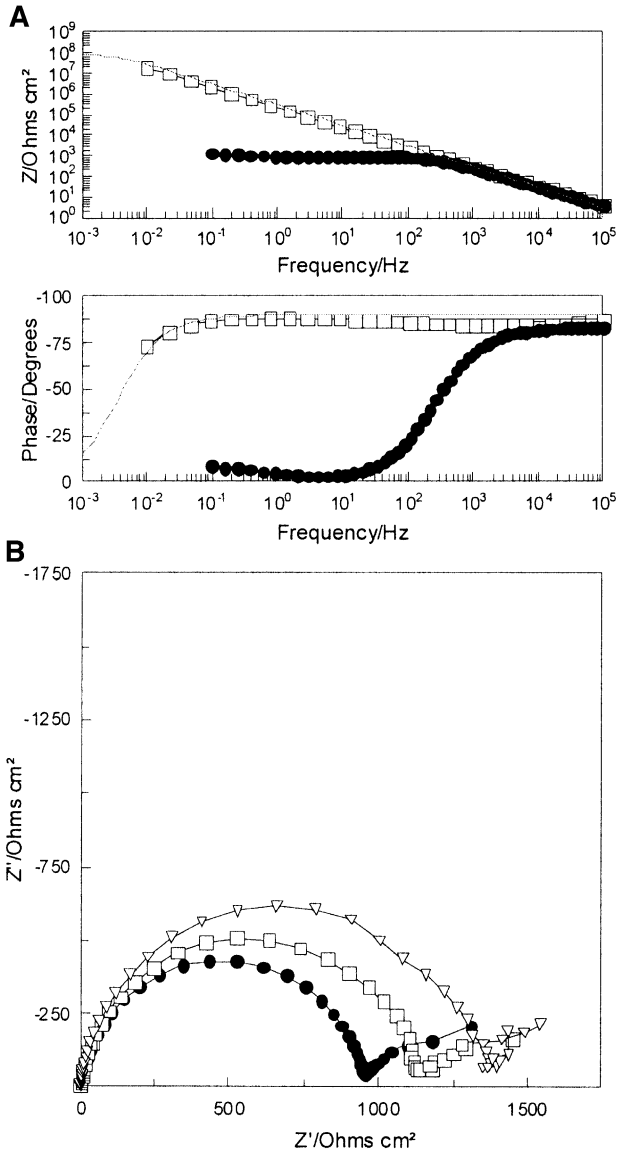

Fig. 5. (A) BODE plots of a DPhyPC membrane on recrystallized SbpA with (circles, filled) and without (squares, open) alamethicin [1 μg/ml] in the presence of 50 mM NaCl, 10 mM Tris, pH 7.5. The solid line represents the simulation curve of the alamethicin-free membrane: Cm (fitted)=0.54 μF/cm^2, Rm (simulated)=80 MΩ cm^2. (B) Inhibition of reconstituted alamethicin ion channels with 5-(*N*-ethyl-*N*-isopropyl)-amiloride. Inhibitor concentration/membrane resistance Rm: 0 μM/954 Ω cm^2 (circles, filled), 10 μM/1121 Ω cm^2 (squares, open) and 20 μM/1311 Ω cm^2 (triangles, open).

Table 1
Summary of the electrochemical parameters of S-layer-supported, painted and folded DPhyPC and MPL membranes

Lipid	Solvent	Support	Cm [μF/cm^2]	Rm [MΩ cm^2]	Conductivity at 0.1 Hz [μS/cm^2]	d [nm]
Electrochemical impedance spectroscopy						
DPhyPC	*n*-hex/EtOH	SbpA ($n=19$)	0.53 ± 0.14	5.0–80	0.36–0.61	3.5 ± 0.7
MPL	*n*-hex/EtOH	SbpA ($n=6$)	0.75 ± 0.07	0.9–60	0.64–1.7	2.5 ± 0.2
MPL	*n*-hex/EtOH	SbpA, GA fix. ($n=5$)	0.74 ± 0.07	1.5–55	0.58–1.05	2.5 ± 0.2
DPhyPC	*n*-hex/EtOH	SUM ($n=6$)	0.69 ± 0.04	25–50	0.49–0.63	2.7 ± 0.2
MPL	*n*-hex/EtOH	SUM ($n=12$)	0.77 ± 0.08	5–55	0.59–0.76	2.4 ± 0.2
MPL	*n*-hex/EtOH	MFM ($n=3$)	0.75 ± 0.03	0.23–25	0.62–4.3	2.5 ± 0.1
Voltage clamp						
DPhyPC [12]	*n*-hex/EtOH	SUM	0.62 ± 0.03			3.0 ± 0.2
MPL [12]	*n*-hex/EtOH	SUM	0.76 ± 0.01			2.4 ± 0.1
DPhyPC [12]	*n*-hex/EtOH	folded BLM	0.64 ± 0.04			2.9 ± 0.2
DPhyPC [41]	*n*-decane	painted BLM	0.41			4.5
DPhyPC [41]	squalene	painted BLM	~ 0.7			2.6–3.0
MPL [41]	*n*-decane	painted BLM	0.74			2.5–3.0

In contrast to DPhyPC bilayers, membrane-spanning MPL monolayers exhibited almost the same specific capacitances Cm ranging from ~ 0.74 to ~ 0.77 μF/cm^2 on SbpA, GA-fixed SbpA, SUM and MFM supports (Table 1). The calculated thickness for all MPL monolayers is ~ 2.5 nm. These data are in good agreement with those of free-standing painted and folded SUM-supported MPL membranes (Table 1). The uniformity in Cm for all MPL membranes strongly indicates a much less pronounced sensitivity against experimental (investigation method), environmental (surface of support) and preparation (solvent) conditions. The latter may be explained that, in contrast to bilayers, MPL membranes are composed of a hydrophobic core without providing a gap for any solvent [41]. The hydrophobic core of a DPhyPC bilayer was found to be thicker than that of tetraetherlipid monolayers [46,47]. Tetraetherlipids may be tilted with respect to the membrane plane, which gives rise to a lower membrane thickness of ~ 2.4 nm [48]. The Rm values of MPL on various supports did not differ very much as well (up to 60 MΩ cm^2). Only MFM-supported MPL membranes exhibited lower resistances (up to 25 MΩ cm^2), although it has to be indicated that only three experiments have been performed. In conclusion, Cm, Rm, and *d* of DPhyPC and MPL membranes supported by various S-layer lattice structures and by MFM are highly comparable to conventional BLMs. Furthermore, although differences in the structure of the DPhyPC and MPL membranes have been observed (Cm, *d*), Rm and the conductivity at 0.1 Hz did not vary significantly for all the investigated membranes resting on the different supports.

3.2.3. Stability and lifetime

The major drawback of free-standing BLMs is their low long-term stability, lasting rarely more than 8 h [49]. A lot of research effort was done on the development of solid-supported, polymer-supported and tethered membranes, which are believed to be the answer to this problem [1,50,51]. Although supported membranes exhibited significant higher mechanical and long-term robustness, the functionality of transmembrane proteins often is impaired, due to a lack of membrane fluidity [52,53] or direct interaction with the solid support [54]. The stability of SbpA- and SUM-supported lipid membranes was investigated with and without insertion of the commonly used membrane-active peptides valinomycin and alamethicin (Table 2). At this point, it should be mentioned that membrane formation and lifetime strongly depended on the quality of the aperture in the plastic sheet. If the rim of the orifice was fringy or badly punched, membrane formation was difficult (or even not feasible) and rupture occurred within 10 min. Generally, in the absence of membrane-active peptides, membranes on untreated SbpA exhibited significant higher long-term stabilities (5–46 h for DPhyPC, 4–44 h for MPL) than those on GA-fixed SbpA (2–18.5 h for MPL) and on SUMs (1–17 h for DPhyPC, 1–18 h for MPL). The voltage-clamp reference data for DPhyPC and MPL supported by a SUM showed a stability of 7.9 +/− 2.4 and 8.3 +/− 2.9 h, respectively, which is for both lipids much lower than the lifetime data obtained by EIS. This clearly demonstrates that also the respective method to investigate the system had an impact on the stability. As mentioned above, MPL membranes on various supports did not vary significantly in their electrochemical parameters; nonetheless, significant deviations in lifetime were observed between membranes on non-modified SbpA and on GA-fixed SbpA. The latter ones exhibited approximately the same long-term stability of ~ 18 h than SUM-supported ones. Accordingly, the maximum lifetime of DPhyPC membranes resting on a SUM was shortened as well (17 h), in comparison to SpbA-supported ones (46 h). This strongly indicated that the increased net-negatively charged GA-fixed SbpA and SUM surfaces apparently affected the lifetime of MPL membranes. Future studies will show if changes in the surface charge of SUMs have an influence on the lifetime. The addition of membrane-active

Table 2
Stability of S-layer-supported lipid membranes with and without reconstituted membrane-active peptides

Lipid	Support	Stability [h]		Reconstituted membrane-active peptides		
		No membrane peptides	With membrane peptides	Valinomycin	Alamethicin	Gramicidin
Electrochemical impedance spectroscopy						
DPhyPC	SbpA	5–46 ($n=6$)	0.5–42 ($n=13$)	yes	yes	yes
MPL	SbpA	4–44 ($n=5$)	2–24 ($n=6$)	yes	yes	yes
MPL	SbpA, GA fix.	2–18.5 ($n=5$)	1–18 ($n=4$)	yes	n.a.	n.a.
DPhyPC	SUM	1–17 ($n=8$)	1–4 ($n=6$)	n.a.	yes	n.a.
MPL	SUM	1–18 ($n=7$)	0.5–18 ($n=8$)	yes	yes	n.a.
Voltage clamp [12]						
DPhyPC	SUM	7.9 ± 2.4				yes
MPL	SUM	8.3 ± 2.9				yes
DPhyPC	folded BLM	6–7				yes

peptides had an influence on the lifetime of DPhyPC and MPL membranes and enhanced the probability for membrane rupture (Table 2). DPhyPC membranes on SbpA with reconstituted valinomycin or alamethicin revealed almost the same lifetime than without the membrane-active peptides, although some broke very shortly after addition of the peptides. However, rupture of DPhyPC membranes resting on a SUM occurred not later than 4 h after alamethicin addition. MPL membranes showed a divergent behaviour upon reconstitution of valinomycin and alamethicin (Table 2). Whereas the lifetime was reduced to one half on the SbpA-support, no effect on the stability due to peptide reconstitution was observed for MPL membranes on GA-fixed SbpA and on SUMs. This provides evidence that the reduction of the lifetime of MPL membranes by surface properties of the support is more serious than possible defects induced by the peptides.

Finally, a broad range of DC bias voltages from −800 to +800 mV was applied to SbpA-supported DPhyPC and MPL membranes and the effect on the membrane capacitance was measured (Fig. 6). All membranes remained very stable as Cm did not change significantly along the voltage spectrum, although no lipids were covalently linked to the supporting layer in contrast to tethered lipid membranes. MPL membranes happened to rupture once in a while at DC bias voltages higher than ±500 mV. By applying a broad range of DC bias voltages on ionophore-containing membranes, the function and the capacity of the subjacent ionic reservoir can be determined [25]. The intrinsic properties of various ionic reservoir types may have a great impact on the conductivity of incorporated ionophores with respect to the ion species [39]. Therefore, the robustness of S-layer-supported membranes against applied DC potentials is very helpful in characterizing the function of the nanoporous S-layer reservoir. Admittedly, for this purpose a different configuration of the measurement cell is required, as the area of the membrane and the porous support should be equal. Therefore, membrane formation on S-layer supports should be performed by vesicle fusion or classic Langmuir and Langmuir–Schaefer techniques instead of the modified Langmuir–Blogdett technique used in the present paper.

3.3. Incorporation of membrane-active molecules

Valinomycin and alamethicin were incorporated to investigate the functionality of S-layer-supported lipid membranes. These membrane-active peptides are well studied and understood and therefore are often used for the characterization and the functionality proof of convenient and supported lipid membranes.

3.3.1. Alamethicin

About 10–20 min after addition of alamethicin at a concentration of 1 μg/ml, the membrane became conductive without application of a DC bias voltage, which was indicated by the drop in the phase angle towards 0° and, thus, a resistive behaviour of the membrane in the middle frequency range (Fig. 5A). The membrane resistance dropped from ~80 MΩ cm^2 to ~950 Ω cm^2, whereas the capacitance did not change. The fraction of the peptide molecules, which inserts in the membrane without an

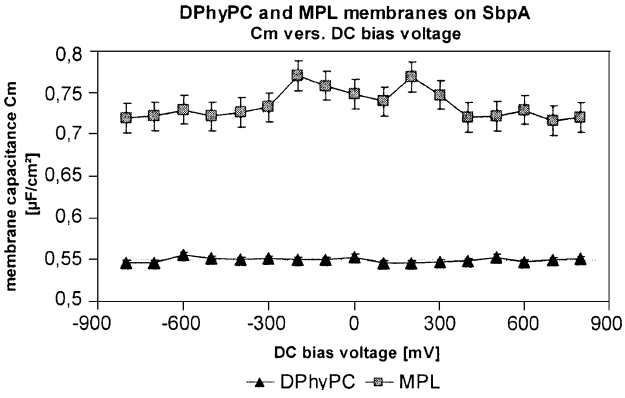

Fig. 6. Membrane capacitance Cm of DPhyPC and a MPL membranes, respectively, on an SbpA support with respect to an applied DC bias voltage from −800 to +800 mV. The error bars for Cm of the DPhyPC membranes are within the width of the triangles.

applied voltage, depends on a critical peptide-to-lipid ratio and on the used lipid (for DPhyPC 1/40) [55]. After alamethicin incorporation, inhibitor was added to the solution (Fig. 5B). The inhibition of alamethicin-mediated conductance of tethered membranes with the sodium channel blocker amiloride and analogues was recently published [56]. Partial inhibition of alamethicin channels with 5-(*N*-ethyl-*N*-isopropyl)-amiloride at a DC bias voltage of 0 mV is shown in Fig. 5B. With increasing amount of inhibitor (in 10 μM steps), the specific resistance of the SbpA-supported DPhyPC-membrane increased to 1120 Ω cm^2 (10 μM) and 1310 Ω cm^2 (20 μM).

In another experiment, the effect of an applied DC bias voltage on alamethicin channels (c = 0.1 μg/ml), which were reconstituted into an MPL-membrane supported by an SbpA-lattice, was demonstrated (Fig. 7A). Alamethicin-mediated conductance already was observed in the absence of an electric field (DC bias voltage = 0 mV). An applied DC bias voltage boosted insertion and ion channel formation. In the presence of an electric field, single alamethicin peptide strands reorientated to form an ion channel [57–59] and caused a decrease in membrane resistance. With increasing applied potential, an increase in the ohmic influence was observed (see Fig. 7A). The major effect was obtained at the application of the first DC bias voltage (− 5 mV) after measuring at zero DC bias voltage. An inductive behaviour of the system is indicated by the loop-like form of the curve in the lower frequency domain, which was interpreted to be a current overcompensation effect [40]. Blocking of alamethicin channels reconstituted in an SbpA-supported MPL-membrane with amiloride–HCl·H_2O, measured at a DC bias voltage of 0 mV, was successful as well (Fig. 7B). Stepwise addition of inhibitor caused a partial blocking of the channels resulting in an increase in Rm.

In conclusion, the incorporation of alamethicin channels could be demonstrated as DPhyPC and MPL membranes already became conductive in the absence of an applied DC bias voltage. Application of DC bias voltages enhanced channel formation and, thus, a decrease in Rm was observed. The successful inhibition of alamethicin channels with two kinds of amiloride inhibitors (5-(*N*-ethyl-*N*-isopropyl)-amiloride and amiloride–HCl·H_2O) provided evidence that, as a matter of principle, S-layer-supported membranes are highly qualified for screening tests on pharmaceutical molecules.

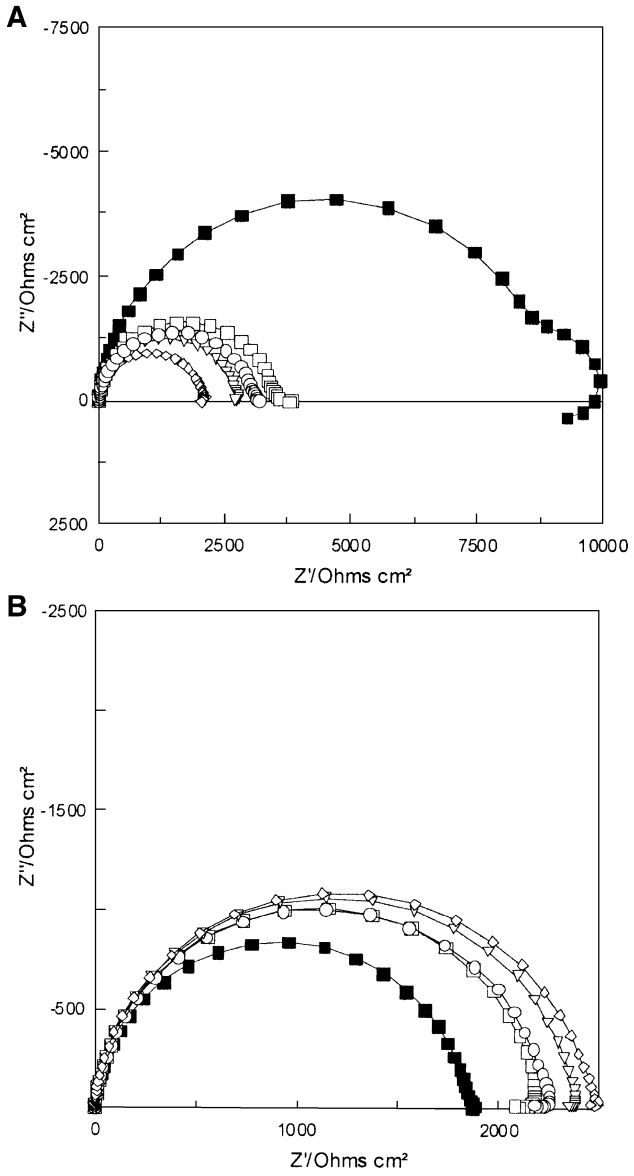

Fig. 7. (A) Voltage-dependent insertion of alamethicin channels (c = 0.1 μg/ml) into MPL-membranes resting on an SbpA covered gold electrode. Electrolyte: 50 mM NaCl, 10 mM Tris, pH 7.5; 30 min after addition, DC bias voltage (DCBV) = 0 mV (squares, filled), DCBV = − 5 mV (squares, open), DCBV = − 25 mV (circles, open), DCBV = − 50 mV (triangles, open) and DCBV = − 100 mV (diamonds, open). (B) Inhibition of alamethicin channels with amiloride–HCl·H_2O; DCBV = 0 mV. Inhibitor concentration/membrane resistance Rm: 0 μM/1786 Ω cm^2 (squares, filled), 20 μM/2099 Ω cm^2 (squares, open), 30 μM/2145 Ω cm^2 (circles, open), 50 μM/2278 Ω cm^2 (triangles, open), 60 μM/2362 Ω cm^2 (diamonds, open).

3.3.2. Valinomycin

The antibiotic polypeptide-like carrier valinomycin shows a distinct transport selectivity for K^+ over Na^+ [60–62]. The selective potassium-transport across a MPL membrane supported by a GA-fixed SbpA was monitored (Fig. 8). After membrane formation, a solution of valinomycin at a concentration of 4×10^{-7} M was added to the buffer, containing 50 mM NaCl, 10 mM Tris, pH 7.5. The membrane resistance dropped from ~ 30 to ~ 17.4 MΩ cm^2. After addition of 50 mM potassium chloride into the buffer, the membrane immediately became conductive (Rm = 42.5 kΩ cm^2), due to the much higher transport efficiency of valinomycin for K^+ ions. The K^+/Na^+ ratio of the valinomycin-mediated ion transport across the MPL membrane was calculated to be 410. This observed K^+/Na^+ transport ratio is not only in good agreement with data obtained with BLMs [63,64], but also with tethered lipid membranes as a reconstitution matrix for valinomycin [25]. Consequently, the biomimetic applicability of S-

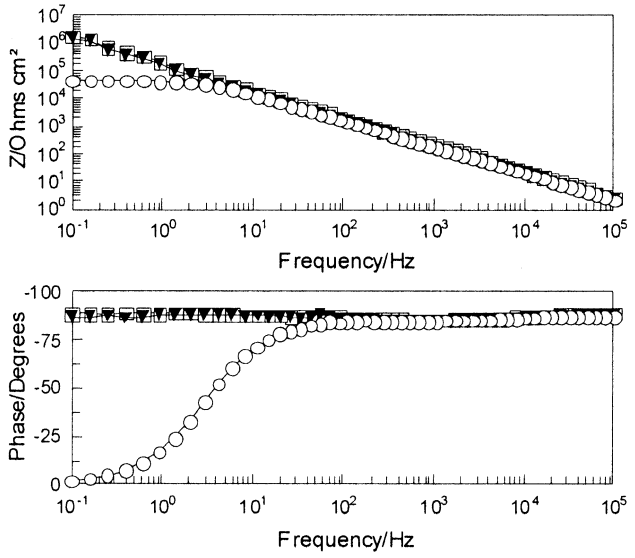

Fig. 8. MPL-membrane on glutaraldehyde-fixed SbpA with (triangles, filled) and without (squares, open) valinomycin at a concentration of 4×10^{-7} M in 50 mM NaCl, 10 mM Tris, pH 7.5. In a further set of experiments, 50 mM KCl (circles, open) was added into the buffer. The K^+/Na^+ ratio of valinomycin-mediated membrane conductance was 410.

layer supported membranes for studying membrane processes was shown by valinomycin-operated selective ion transport.

Impedance measurements also were performed with gramicidin. The functionality of this membrane-active peptide was approved. These data will be published in a separate paper together with other currently ongoing studies on gramicidin.

4. Conclusion

In the present study, the suitability of EIS as a transducer principle in determining the electrochemical properties of S-layer supported DPhyPC and MPL membranes was demonstrated. The insulating properties of phospholipid bilayers and archaeal bolamphiphilic tetraetherlipid membranes supported by various S-layer lattice structures were highly comparable to conventional free-standing lipid membranes. A significant enhancement in long-term robustness was achieved, especially with membranes deposited on recrystallized SbpA lattices. S-layers provided an excellent biochemical environment for the reconstitution of membrane-active molecules such as valinomycin and alamethicin. The major advantage of S-layer proteins recrystallized on metal surfaces over SUMs is their enhanced application potential: The outstanding property of monomeric S-layer proteins is their ability to recrystallize on various surfaces such as silicon, gold and indium-tin-oxide in a large-scale order. Therefore, S-layer subunits are very promising building blocks, particularly with regard to functionalized membranes resting on S-layer-covered photolithographic fabricated microelectrode arrays for medical and pharmaceutical high-throughput-screening devices. It is assumed that the usage of S-layer/streptavidin fusion proteins as a support for biotinylated membranes will lead to an additional improvement in long-term robustness. S-layers are an auspicious alternative to other polymer-cushioned supports [2,52,65]. Another interesting approach would be the application of S-layers as a stabilizing matrix for membranes on a planar "patch clamp on a chip" [66,67]. The present results demonstrate that the implementation of crystalline arrays of S-layer proteins as a hydrophilic, isoporous, water-containing intermediate and stabilizing matrix is a very competitive technology for the development of membrane protein-based biosensors.

Acknowledgements

This work was supported by a grant from the Austrian Science Foundation, Project 14419-MOB and Project 16925-B07, and by the Volkswagen Foundation, Germany, Project I/77710. Jacqueline Friedmann is gratefully acknowledged for assistance with AFM.

References

[1] E. Sackmann, Supported membranes: scientific and practical applications, Science 271 (1996) 43–48.
[2] E. Sackmann, M. Tanaka, Supported membranes on soft polymer cushions: fabrication, characterization and applications, Trends Biotechnol. 18 (2000) 58–64.
[3] A.L. Plant, M. Gueguetschkeri, W. Yap, Supported phospholipid/alkanethiol biomimetic membranes: insulating properties, Biophys. J. 67 (1993) 1126–1133.
[4] E.L. Florin, H.E. Gaub, Painted supported lipid membranes, Biophys. J. 64 (1993) 375–383.
[5] H. Lang, C. Duschl, H. Vogel, A new class of thiolipids for the attachment of lipid bilayers on gold surfaces, Langmuir 10 (1994) 197–210.
[6] J.T. Groves, N. Ulman, S.G. Boxer, Micropatterning fluid lipid bilayers on solid supports, Science 275 (1997) 651–653.
[7] E. Kalb, S. Frey, L.K. Tamm, Formation of supported planar bilayers by fusion of vesicles to supported phospholipid monolayers, Biochim. Biophys. Acta 1103 (1992) 307–316.
[8] B. Wetzer, D. Pum, U.B. Sleytr, S-layer stabilized solid supported lipid bilayers, J. Struct. Biol. 119 (1997) 123–128.
[9] D. Pum, U.B. Sleytr, Molecular nanotechnology and biomimetics with S-layers, in: U.B. Sleytr, P. Messner, D. Pum, M. Sára (Eds.), Crystalline Bacterial Cell Surface Proteins, Academic Press, Austin, TX, 1996, pp. 175–209.
[10] B. Schuster, D. Pum, O. Braha, H. Bayley, U.B. Sleytr, Self-assembled alpha-hemolysin pores in an S-layer-supported lipid bilayer, Biochim. Biophys. Acta 1370 (1998) 280–288.
[11] B. Schuster, D. Pum, M. Sára, O. Braha, H. Bayley, U.B. Sleytr, S-layer ultrafiltration membranes: a new support for stabilizing functionalized lipid membranes, Langmuir 17 (2001) 499–503.
[12] B. Schuster, S. Weigert, D. Pum, M. Sara, U.B. Sleytr, New method for generating tetraether lipid membranes on porous supports, Langmuir 19 (2003) 2392–2397.
[13] U.B. Sleytr, M. Sára, D. Pum, B. Schuster, Molecular nanotechnology and nanobiotechnology with two-dimensional protein crystals (S-layers), in: M. Rosoff (Ed.), Nano-Surface Chemistry, Marcel Dekker, New York, 2001, pp. 333–389.

[14] A. Breitwieser, E.M. Egelseer, D. Moll, N. Ilk, C. Hotzy, B. Bohle, C. Ebner, U.B. Sleytr, M. Sára, A recombinant bacterial cell surface (S-layer)-major birch pollen allergen-fusion protein (rSbsC/Bet v1) maintains the ability to self-assemble into regularly structured monomolecular lattices and the functionality of the allergen, Protein Eng. 15 (2002) 243–249.
[15] D. Moll, C. Huber, B. Schlegel, D. Pum, U.B. Sleytr, M. Sára, S-layer-streptavidin fusion proteins as template for nanopatterned molecular arrays, Proc. Natl. Acad. Sci. U. S. A. 99 (2002) 14646–14651.
[16] M. Pleschberger, A. Neubauer, E.M. Egelseer, S. Weigert, B. Lindner, U.B. Sleytr, S. Muyldermans, M. Sára, Generation of a functional monomolecular protein lattice consisting of an S-layer fusion protein comprising the variable domain of a camel heavy chain antibody, Bioconjug. Chem. 14 (2003) 440–448.
[17] W. Baumeister, G. Lembcke, Structural features of archaebacterial cell envelopes, J. Bioenerg. Biomembr. 24 (1992) 567–575.
[18] T.A. Langworthy, J.L. Pond, Archaebacterial ether lipids and chemotaxonomy, Syst. Appl. Microbiol. 7 (1986) 253–257.
[19] A. Gliozzi, A. Relini, P.L.G. Chong, Structure and permeability properties of biomimetic membranes of bolaform archaeal tetraether lipids, J. Membr. Sci. 206 (2002) 131–147.
[20] N. Ilk, C. Völlenkle, E.M. Egelseer, A. Breitwieser, U.B. Sleytr, M. Sára, Molecular characterization of the S-layer gene, sbpA, of *Bacillus sphaericus* CCM 2177 and production of a functional S-layer fusion protein with the ability to recrystallize in a defined orientation while presenting the fused allergen, Appl. Environ. Microbiol. 68 (2002) 3251–3260.
[21] M. Weygand, B. Wetzer, D. Pum, U.B. Sleytr, N. Cuvillier, K. Kjaer, P.B. Howes, M. Lösche, Bacterial S-layer protein coupling to lipids: X-ray reflectivity and grazing incidence diffraction studies, Biophys. J. 76 (1999) 458–468.
[22] N. Ilk, P. Kosma, M. Puchberger, E.M. Egelseer, H.F. Mayer, U.B. Sleytr, M. Sara, Structural and functional analyses of the secondary cell wall polymer of *Bacillus sphaericus* CCM 2177 that serves as an S-layer-specific anchor, J. Bacteriol. 181 (1999) 7643–7646.
[23] H. Engelhardt, J. Peters, Structural research on surface layers: a focus on stability, surface layer homology domains, and surface layer–cell wall interactions, J. Struct. Biol. 124 (1998) 276–302.
[24] C. Steinem, A. Janshoff, W.P. Ulrich, M. Sieber, H.J. Galla, Impedance analysis of supported lipid bilayer membranes: a scrutiny of different preparation techniques, Biochim. Biophys. Acta 1279 (1996) 169–180.
[25] B. Raguse, V. Braach-Maksvytis, B.A. Cornell, L.G. King, P.D.J. Osman, R.J. Pace, L. Wieczorek, Tethered lipid bilayer membranes: formation and ionic reservoir characterization, Langmuir 14 (1998) 648–659.
[26] R. Naumann, E.K. Schmidt, A. Jonczyk, K. Fendler, B. Kadenbach, T. Liebermann, A. Offenhaeusser, W. Knoll, The peptide-tethered lipid membrane as a biomimetic system to incorporate cytochrome *c* oxidase in a functionally active form, Biosens. Bioelectron. 14 (1999) 651–662.
[27] S. Gritsch, P. Nollert, F. Jahnig, E. Sackmann, Impedance spectroscopy of porin and gramicidin pores reconstituted into supported lipid bilayers on indium-tin-oxide electrodes, Langmuir 14 (1998) 3118–3125.
[28] O. Purrucker, H. Hillebrandt, K. Adlkofer, M. Tanaka, Deposition of highly resistive lipid bilayer on silicon-silicon dioxide electrode and incorporation of gramicidin studied by ac impedance spectroscopy, Electrochim. Acta 47 (2001) 791–798.
[29] U.B. Sleytr, M. Sára, Ultrafiltration membranes with uniform pores from crystalline bacterial cell envelope layers, Appl. Microbiol. Biotechnol. 25 (1986) 83–90.
[30] M. Sára, U.B. Sleytr, Production and characteristics of ultrafiltration membranes with uniform pores from two-dimensional arrays of proteins, J. Membr. Sci. 33 (1987) 27–49.
[31] U.B. Sleytr, M. Sára, Z. Küpcü, P. Messner, Structural and chemical characterization of S-layers of selected strains of *Bacillus stearothermophilus* and *Desulfotomaculum nigrificans*, Arch. Microbiol. 146 (1986) 19–24.
[32] S. Weigert, M. Sára, Surface modification of an ultrafiltration membrane with crystalline structure and studies on the interactions with selected protein molecules, J. Membr. Sci. 106 (1995) 147–159.
[33] D.P. Nikolelis, U.J. Krull, Reliable and facile method for preparation of solventless bilayer lipid membranes for electroanalytical investigations, Talanta 39 (1992) 1045–1049.
[34] J.R. Macdonald, Impedance Spectroscopy, Wiley, New York, 1987.
[35] C. Steinem, A. Janshoff, F. Hoehn, M. Sieber, H.J. Galla, Proton translocation across bacteriorhodopsin containing solid supported lipid bilayers, Chem. Phys. Lipids 89 (1997) 141–152.
[36] A. Abdelghani, C. Jacquin, M. Huber, R. Deutschmann, E. Sackmann, Supported lipid membrane on semiconductor electrode, Mater. Chem. Phys. 70 (2001) 187–190.
[37] R. Naumann, S.M. Schiller, F. Giess, B. Grohe, K.B. Hartmann, I. Kärcher, I. Köper, J. Lübben, K. Vasilev, W. Knoll, Tethered lipid bilayers on ultraflat gold surfaces, Langmuir 19 (2003) 5435–5443.
[38] B.A. Cornell, G. Krishna, P.D. Osman, R.D. Pace, L. Wieczorek, Tethered-bilayer lipid membranes as a support for membrane-active peptides, Biochem. Soc. Trans. 29 (2001) 613–617.
[39] G. Krishna, J. Schulte, B.A. Cornell, R. Pace, L. Wieczorek, P.D. Osman, Tethered bilayer membranes containing ionic reservoirs: the interfacial capacitance, Langmuir 17 (2001) 4858–4866.
[40] K.D. Schulze, H. Herrnberger, Impedance spectroscopic investigation of ion channel formation in lipid membranes, Z. Phys. Chem. 194 (1996) 243–254.
[41] J. Stern, H.J. Freisleben, S. Janku, K. Ring, Black lipid membranes of tetraether lipids from *Thermoplasma acidophilum*, Biochim. Biophys. Acta 1128 (1992) 227–236.
[42] C. Miller, Ion Channel Reconstitution, Plenum, New York, 1986.
[43] S.H. White, Formation of "solvent-free" black lipid bilayer membranes from glyceryl monooleate dispersed in squalene, Biophys. J. 23 (1978) 337–347.
[44] S.H. White, D.C. Petersen, S. Simon, M. Yafuso, Formation of planar bilayer membranes from lipid monolayers. A critique, Biophys. J. 16 (1976) 481–489.
[45] W. Hanke, W.-R. Schlue, Planar Lipid Bilayers, Academic Press, San Diego, 1993.
[46] U. Bakowsky, U. Rothe, E. Antonopoulos, T. Martini, L. Henkel, H.J. Freisleben, Monomolecular organization of the main tetraether lipid from *Thermoplasma acidophilum* at the water–air interface, Chem. Phys. Lipids 105 (2000) 31–42.
[47] A. Gliozzi, M. Robello, L. Fittabile, A. Relini, A. Gambacorta, Valinomycin acts as a channel in ultrathin lipid membranes, Biochim. Biophys. Acta 1283 (1996) 1–3.
[48] L. Fittabile, M. Robello, A. Relini, M. De Rosa, A. Gliozzi, Organization of monolayer-formed membranes made from archeal ether lipids, Thin Solid Films 284–85 (1996) 735–738.
[49] H. Ti Tien, A. Ottova, From self-assembled bilayer lipid membranes (BLMs) to supported BLMs on metal and gel substrates to practical applications, Colloids Surf., A Physicochem. Eng. Asp. 149 (1999) 217–233.
[50] H.M. McConnell, T.H. Watts, R.M. Weis, A.A. Brian, Supported planar membranes in studies of cell–cell recognition in the immune system, Biochim. Biophys. Acta 864 (1986) 95–106.
[51] E.K. Sinner, W. Knoll, Functional tethered membranes, Curr. Opin. Chem. Biol. 5 (2001) 705–711.
[52] M.L. Wagner, L.K. Tamm, Tethered polymer-supported planar lipid bilayers for reconstitution of integral membrane proteins: silane-polyethyleneglycol-lipid as a cushion and covalent linker, Biophys. J. 79 (2000) 1400–1414.
[53] C.A. Naumann, O. Prucker, T. Lehmann, J. Ruhe, W. Knoll, C.W. Frank, The polymer-supported phospholipid bilayer: tethering as a new approach to substrate-membrane stabilization, Biomacromolecules 3 (2002) 27–35.

[54] J. Salafsky, J.T. Groves, S.G. Boxer, Architecture and function of membrane proteins in planar supported bilayers: a study with photosynthetic reaction centers, Biochemistry 35 (1996) 14773–14781.
[55] K. He, S.J. Ludtke, W.T. Heller, H.W. Huang, Mechanism of alamethicin insertion into lipid bilayers, Biophys. J. 71 (1996) 2669–2679.
[56] P. Yin, C.J. Burns, P.D.J. Osman, B.A. Cornell, A tethered bilayer sensor containing alamethicin channels and its detection of amiloride based inhibitors, Biosens. Bioelectron. 18 (2003) 389–397.
[57] D.P. Tieleman, H.J. Berendsen, M.S. Sansom, An alamethicin channel in a lipid bilayer: molecular dynamics simulations, Biophys. J. 76 (1999) 1757–1769.
[58] H. Duclohier, H. Wroblewski, Voltage-dependent pore formation and antimicrobial activity by alamethicin and analogues, J. Membr. Biol. 184 (2001) 1–12.
[59] M. Eisenberg, J.E. Hall, C.A. Mead, The nature of the voltage-dependent conductance induced by alamethicin in black lipid membranes, J. Membr. Biol. 14 (1973) 143–176.
[60] M. Dobler, Ionophores and their Structures, Wiley-Interscience, New York, 1981, pp. 39–51.
[61] C. Steinem, A. Janshoff, B.K. Von Dem, K. Reihs, J. Goosssens, H.J. Galla, Valinomycin-mediated transport of alkali cations through solid supported membranes, Bioelectrochem. Bioenerg. 45 (1998) 17–26.
[62] G. Favero, L. Campanella, A. D'Annibale, R. Santucci, T. Ferri, Mixed hybrid bilayer lipid membrane incorporating valinomycin: improvements in preparation and functioning, Microchem. J. 74 (2002) 141–148.
[63] G. Stark, Carrier-mediated ion transport across thin lipid membranes, in: G. Giebisch, D.C. Tosteson, H. Ussing (Eds.), Membrane Transport in Biology, vol. 1. Springer, Berlin, 1978, pp. 447–473.
[64] P. Läuger, Mechanismen des biologischen Ionentransports—Carrier, Kanäle und Pumpen in künstlichen Lipidmembranen, Angew. Chem. 97 (1985) 939–959.
[65] H. Hillebrandt, G. Wiegand, M. Tanaka, E. Sackmann, High electric resistance polymer/lipid composite films on indium-tin-oxide electrodes, Langmuir 15 (1999) 8451–8459.
[66] K.G. Klemic, J.F. Klemic, M.A. Reed, F.J. Sigworth, Micromolded PDMS planar electrode allows patch clamp electrical recordings from cells, Biosens. Bioelectron. 17 (2002) 597–604.
[67] N. Fertig, M. Klau, M. George, R.H. Blick, J.C. Behrens, Activity of single ion channel proteins detected with a planar microstructure, Appl. Phys. Lett. 81 (2002) 4865–4867.